Journal of Organometallic Chemistry 902 (2019) 120962

Contents lists available at ScienceDirect

Journal of Organometallic Chemistry

journal homepage: www.elsevier.com/locate/jorganchem

Stereochemistry of oxidative addition of methyl iodide and hydrogen peroxide to organoplatinum(II) complexes having an appended phenol group and the supramolecular chemistry of the platinum(IV) products

Ava Behnia, Mahmood Azizpoor Fard, Richard J. Puddephatt*

Department of Chemistry, University of Western Ontario, London, N6A 5B7, Canada

ARTICLE INFO

Article history:
Received 23 August 2019
Received in revised form
25 September 2019
Accepted 26 September 2019
Available online 27 September 2019

Keywords:
Platinum
Oxidative addition
Cycloneophyl
Methyl iodide
Hydrogen peroxide

ABSTRACT

The oxidative addition chemistry of cycloneophylplatinum (II) complexes containing ligands with an appended phenol group is reported. The platinum (II) complexes [Pt ($CH_2CMe_2C_6H_4$) (**L**)] with **L** = 2-C_6H_4NCH=N-2-C_6H_4OH (**L1**) or 2-$C_6H_4NCH_2$−NH-n-C_6H_4OH (**L2**, n = 2; **L3**, n = 3; **L4**, n = 4) react with MeI or H_2O_2 to give the corresponding platinum (IV) complexes [PtIMe($CH_2CMe_2C_6H_4$) (**L**)] or [Pt ($OH)_2$($CH_2CMe_2C_6H_4$) (**L**)], respectively. NMR studies indicate that methyl iodide initially gives *trans* oxidative addition, but the initial products isomerize rapidly, often to give complex mixtures. The crystalline products all have structures with *cis* orientation of the PtIMe unit, whose formation is thought to require two isomerization steps after the initial oxidative addition. In contrast, the oxidative addition of H_2O_2 occurs with trans stereochemistry and no subsequent isomerization is observed. The iodoplatinum (IV) complexes [PtIMe($CH_2CMe_2C_6H_4$) (**L**)] form intramolecular OH·I hydrogen bonds (**L1**) or intermolecular OH·I hydrogen bonds to give head-to-tail dimers (**L2** or **L4**), or a hydrogen bond to solvent (**L3**). The complex [Pt ($OH)_2$($CH_2CMe_2C_6H_4$) (**L4**)] forms an unusual racemic supramolecular polymer with multiple OH·O and NH O hydrogen bonds.

© 2019 Elsevier B.V. All rights reserved.

1. Introduction

The oxidative addition reaction often constitutes a key bond activation step in homogeneous catalysis and so major efforts have been made to understand the factors that control reactivity and stereochemistry in these reactions [1–6]. The recent advances in cooperative catalysis, combining transition metal catalysis and organocatalysis for example, makes it important to understand how typical organic functional groups used in organocatalysis might affect the key steps in transition metal complex catalysis [7–10]. Because alkylplatinum bonds are relatively inert towards protic reagents, the organometallic complexes of platinum are particularly well suited to studies of oxidative addition in the presence of protic solvents or with ligands having appended hydroxyl group functionality [11–16]. The hydroxyl groups can promote oxidation of platinum (II) to platinum (IV) on reaction with dioxygen and this is important in studies of conversion of methane to methanol [11–16]. Hydrogen bonding can play an important role in promoting reactivity and it can also control the supramolecular chemistry of the organoplatinum (IV) products [11–20].

This paper will report on some oxidative addition chemistry of cycloneophylplatinum (II) complexes containing ligands with an appended phenol group [21–23]. The platinum (II) complexes **1**–**4** (Chart 1) have been reported recently [21]. Complexes **1** and **2** were shown to contain an intramolecular OH Pt hydrogen bond and it was of interest to determine how this unusual bond affected the oxidative addition chemistry.

2. Results and discussion

2.1. Structure of the ligand *L2*

The ligands **L2** − **L4** used in this research contain both NH and OH groups that might act as hydrogen bond donors [21]. The structure of **L2** was determined and is shown in Fig. 1. The hydrogen bonding occurs between the phenol group as donor and the pyridyl

* Corresponding author.
E-mail address: pudd@uwo.ca (R.J. Puddephatt).

https://doi.org/10.1016/j.jorganchem.2019.120962
0022-328X/© 2019 Elsevier B.V. All rights reserved.

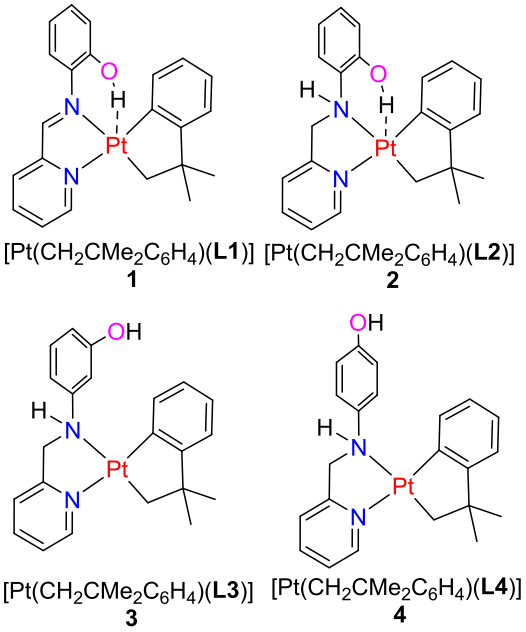

Chart 1. The cycloneophylplatinum (II) complexes, [Pt ($CH_2CMe_2C_6H_4$) (**L**)], **1**–**4**, with ligands **L1** – **L4**, respectively.

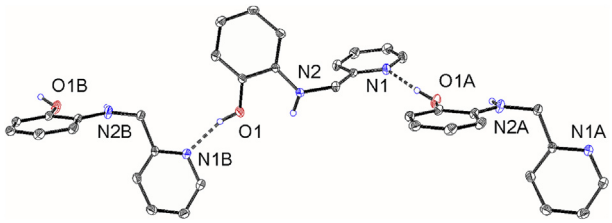

Fig. 1. The structure of the ligand **L2**, showing 40% probability ellipsoids. Selected distances: O (1)-H (1H) 0.88 (2), N (1B)–H (1H) 1.85 (3), O (1) N (1B) 2.697 (1), N (2)-H (2 N) 0.90 (2) Å; O (1)-H (1H)–N (1B) 161 (2)°. Symmetry equivalent atoms: x, y, z; A, x-½, ½-y, z-1; B, ½+x, 1/2 -y, 1 + z.

group as acceptor and gives rise to a supramolecular polymer. The neighboring molecules are related by mirror symmetry so, although each molecule is chiral because of the dissymmetric N (2) center, the polymer is racemic. The NH group is not involved in hydrogen bonding (the intramolecular distance N (2)H (2 N) O (1) is 2.17 (2) Å), though there will be a weak dipole-dipole attraction.

2.2. Oxidative addition of methyl iodide

The reaction of complex **1** with methyl iodide in dichloromethane at room temperature occurred with precipitation of the yellow platinum (IV) complex [PtIMe($CH_2CMe_2C_6H_4$) (**L1**)], **5a**, Scheme 1, whose structure is shown in Fig. 2. The complex has octahedral stereochemistry and there is an intramolecular OH I hydrogen bond with distance O (1) I (1) of 3.49 Å. The most notable feature of the structure of **5a** is that the methyl and iodide ligands are mutually *cis*, whereas most oxidative addition reactions of methyl iodide occur by the S_N2 mechanism and give *trans* stereochemistry [1–6]. The ^{1}H NMR spectrum of **5a** in dmso-d_6 indicated that a single isomer, with no symmetry, was present. Thus, two resonances were observed for each of the CH_2 and CMe_2 groups of the cycloneophyl group. The imine resonance of **5a** was observed at δ 9.18, with $^3J_{PtH} = 33$ Hz, and the methylplatinum resonance was at

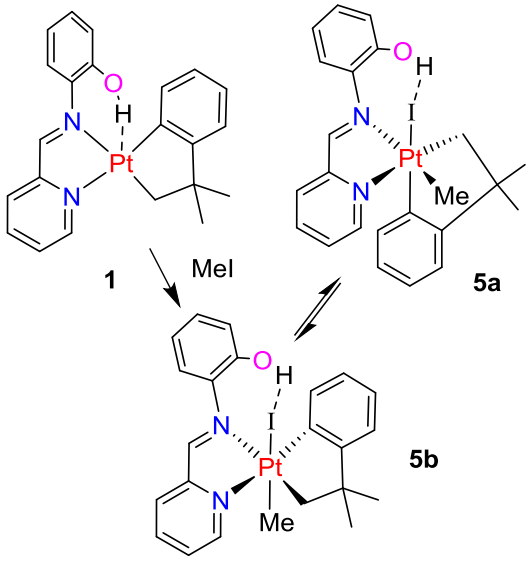

Scheme 1. Reaction of complex **1** with methyl iodide.

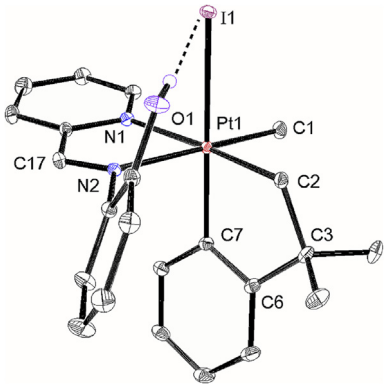

Fig. 2. A view of the structure of complex **5a**, showing 30% probability ellipsoids. Selected bond parameters: Pt (1)C (1) 2.052 (2), Pt (1)C (2) 2.049 (2), Pt (1)C (7) 2.011 (2), Pt (1)N (1) 2.174 (2), Pt (1)N (2) 2.175 (2), Pt (1)I (1) 2.7466 (12) Å; C (2)Pt (1)C (7) 82.18 (10), N (1)Pt (1)N (2) 76.45 (8) °.

δ 1.47, with $^2J_{PtH} = 72$ Hz. Because the stereochemistry of complex **5a** was unexpected, a reaction of complex **1** with CD_3I in CD_2Cl_2 solution was carried out at low temperature and monitored by NMR spectroscopy. Reaction occurred slowly at −20 °C to give a new isomer **5b**-d_3, as indicated in the ^{1}H NMR spectrum by decay of the imine resonance of complex **1** at δ 9.38, with $^3J_{PtH} = 27$Hz, and growth of a new imine resonance at δ 8.91, with $^3J_{PtH} = 24$ Hz. The reaction was complete at 0 °C and complete NMR data were obtained at this temperature. In a similar reaction using MeI, the methylplatinum resonance of **5b** was observed at δ 0.87, with $^2J_{PtH} = 72$ Hz. This isomer **5b** was soluble in CD_2Cl_2 but, on warming above 0 °C, an insoluble precipitate was formed and shown to be **5a** by its ^{1}H NMR spectrum in dmso-d_6. The NMR data do not define the stereochemistry of **5b**, and it was not possible to grow crystals of this isomer, so the proposed stereochemistry resulting from *trans* oxidative addition is less certain than for the crystallographically characterized isomer **5a**. However, the proposed structure **5b** is supported by the upfield chemical shift of the methylplatinum resonance [6,12]. There are six potential isomers of complex **5**, with the favored *fac*-PtC_3 coordination, but only two (**5a** and **5b**) were observed.

Oxidative addition of methyl iodide to the platinum (II) complexes **2**–**4** all gave crystalline platinum (IV) complexes which were characterized crystallographically as **6a** – **8a** (Scheme 2, Figs. 3–5). Remarkably, the molecular structures are similar to each other and also to complex **5a** (Fig. 2), with methyl *trans* to amine, CH_2 *trans* to pyridine, and C_6H_4 *trans* to iodide, corresponding to a product of *cis* oxidative addition. With the amine ligands, there are twelve possible geometrical isomers, compared to six with the imine ligand, because either the NH or N-phenol group can be *syn* or *anti* to the Pt–I group. In all complexes **6a** – **8a**, the NH group is *syn* to the Pt–I group (Scheme 2, Figs. 3–5). In the structure of complex **6a** (Fig. 3), the *anti* arrangement of the 2-phenol group to the Pt–I group does not allow formation of an intramolecular OH IPt hydrogen bond like that found in **5a** (Fig. 2), but pairwise weak intermolecular OH IPt hydrogen bonds are formed with a neighboring molecule instead, with O (1) I (1A) = I (1) O (1A) = 3.43 (1) Å. The two molecules are related by an inversion center, so they make a racemic pair (Fig. 3). The structure of complex **7a** is shown in Fig. 4. In the lattice of this complex, there is a molecule of acetone and the phenol group forms an OH O=CMe_2 hydrogen bond to the solvate molecule [O (1) O (1S) = 2.83 Å], and not the OH IPt bond observed with the other complexes. There are equal numbers of molecules related by inversion symmetry, and the lattice is not chiral. As shown in Fig. 5, complex **8a** forms a head-to-tail dimer by forming intermolecular OH IPt hydrogen bonds, with distance O I 3.52 (1) Å, representing a weak hydrogen bond [24,25]. As in complex **6a** (Fig. 3), the two molecules in the dimer are related by inversion symmetry. In all complexes **6a** – **8a** the Pt–N (amine) bond is significantly longer than the Pt–N (pyridine) bond (Figs. 3–5).

Although the structures of **6a** – **8a** are all of the same isomeric form (Scheme 2, Figs. 3–5), the ^{1}H NMR spectra indicated that a complex mixture of isomers was present in solution. A study of the reactions of complexes **2**–**4** with CD_3I at low temperature was therefore carried out to gain insight into the course of the reactions. In each case, a major isomer was formed at about −20 °C along with two or three minor isomers and, on warming to room temperature, a more complex mixture of isomers was formed. In this case, it seems that the rate of isomerization is competitive with the rate of oxidative addition, and that several isomers have similar energies, so it is remarkable that the single crystals all have the same isomeric form.

The stereochemistry of the above oxidative addition reactions with methyl iodide was not easily predicted and some further discussion is warranted. For the diimine complex **1**, both the oxidative addition and isomerization reactions are expected to occur by way of ionic 5-coordinate square pyramidal intermediates [PtMe($CH_2CMe_2C_6H_4$) (**L1**)]$^+$I$^-$, formed in the S_N2 mechanism of

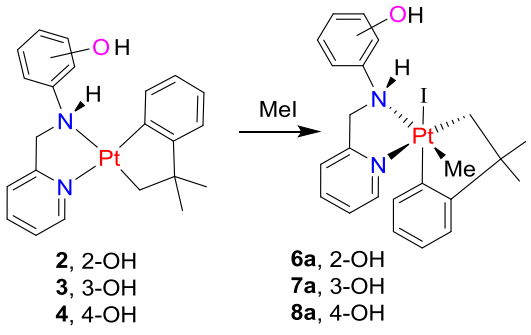

Scheme 2. Formation of platinum (IV) complexes [PtIMe($CH_2CMe_2C_6H_4$) (**L**)], L = **L2**-**L4**.

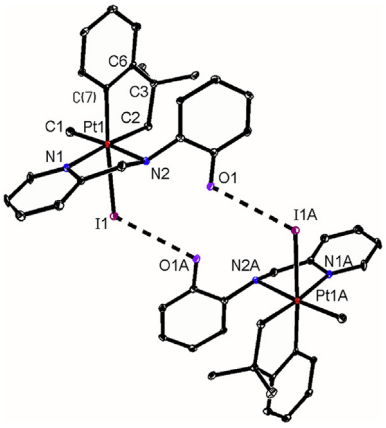

Fig. 3. A view of the structure of complex **6a**, showing 30% probability ellipsoids. Selected bond parameters: Pt (1)C (1) 2.061 (6), Pt (1)C (2) 2.048 (5), Pt (1)C (7) 2.006 (5), Pt (1)N (1) 2.177 (4), Pt (1)N (2) 2.247 (5), Pt (1)I (1) 2.7510 (8) Å; C (2)Pt (1)C (7) 82.9 (2), N (1)Pt (1)N (2) 78.35 (17) °. Symmetry related atoms are related by coordinates x, y, z; 1-x, -y, 1-z.

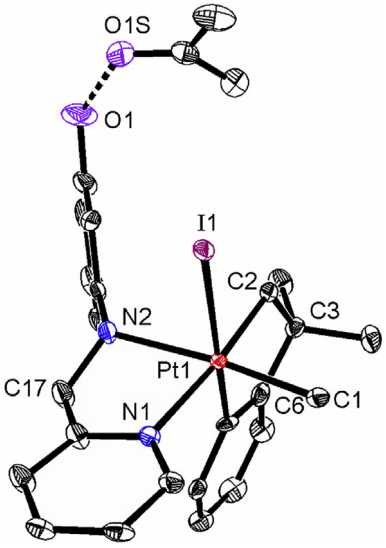

Fig. 4. A view of the structure of complex **7a**, showing 30% probability ellipsoids. Selected bond parameters: Pt (1)C (1) 2.049 (7), Pt (1)C (2) 2.045 (6), Pt (1)C (7) 1.994 (6), Pt (1)N (1) 2.182 (5), Pt (1)N (2) 2.238 (5), Pt (1)I (1) 2.7541 (9) Å; C (2)Pt (1)C (7) 82.7 (3), N (1)Pt (1)N (2) 75.97 (19) °.

oxidative addition or, for the isomerization steps, by reversible dissociation of an iodido ligand from the expected kinetic product of oxidative addition **5b** (Schemes 1 and 3) [6,21,26]. For isomerization from **5b**, dissociation of an iodido ligand occurs to give **5b**$^+$ and then one of the equatorial groups (CH_2 to give **5c**$^+$ or C_6H_4 to give **5d**$^+$) moves to the vacant site, the methyl group moves from the axial site to the vacated equatorial site, and then the iodide recoordinates. This would give **5c** (CH_2 migration) or **5d** (C_6H_4 migration) as shown in Scheme 3, but not **5a**. One more isomerization step from **5c**, involving dissociation of the iodido ligand, migration of the CH_2 and C_6H_4 groups and iodide coordination, can give the observed product **5a**. The complete sequence showing how the six isomers **5a** – **5f** might be formed is shown in Scheme 4.

The DFT calculated structures of the six possible isomers of **5** are shown in Fig. 6. The isomers **5a** and **5e** are calculated to be equally stable, but there was no experimental evidence for formation of **5e**. The most reasonable explanation is that the activation energy to

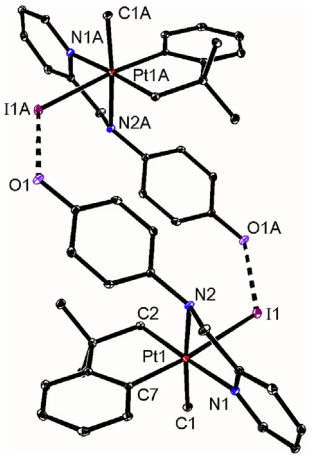

Fig. 5. A view of the structure of complex **8a**, showing 30% probability ellipsoids. Selected bond parameters: Pt (1)C (1) 2.056 (3), Pt (1)C (2) 2.052 (3), Pt (1)C (7) 2.007 (3), Pt (1)N (1) 2.174 (3), Pt (1)N (2) 2.242 (3), Pt (1)I (1) 2.7824 (12) Å; C (2)Pt (1)C (7) 82.29 (13), N (1)Pt (1)N (2) 77.24 (10) °. Symmetry related atoms are related by the coordinates x, y, z; 1-x, 2-y, 1-z.

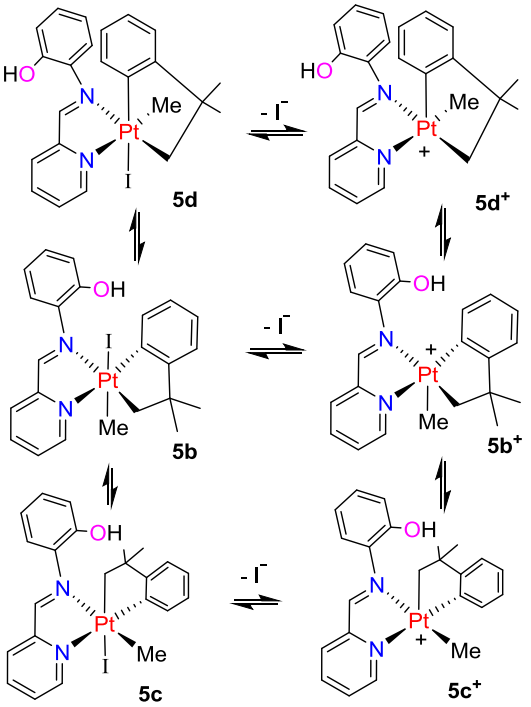

Scheme 3. The predicted mechanism of isomerization of **5b** to give **5c** or **5d**, via the square pyramidal cationic intermediates **5b**$^{+}$, **5c**$^{+}$ and **5d**$^{+}$.

form **5a** is lower and, once formed, it does not react further. However, with available resources, the system is too complex to allow transition states to be found [26].

For complexes **6a** – **8a**, another challenge is to understand why the *syn* orientation of iodide and NH groups is observed in the isolated products (Figs. 3–5). DFT calculations predict that **6a** is more stable than the structure **6a′**, with *anti* orientation of iodide and NH groups, by 6 kJ mol^{-1} (Fig. 7). This might be attributed to steric effects or to the shorter attractive NH$^{\delta+}$/PtI$^{\delta-}$ interaction in **6a** outweighing the less favorable OH IPt interaction. Similarly, for the expected kinetic products of *trans* oxidative addition, **6b** is predicted to be 8 kJ mol^{-1} lower in energy than **6b'** (Fig. 7). However, in

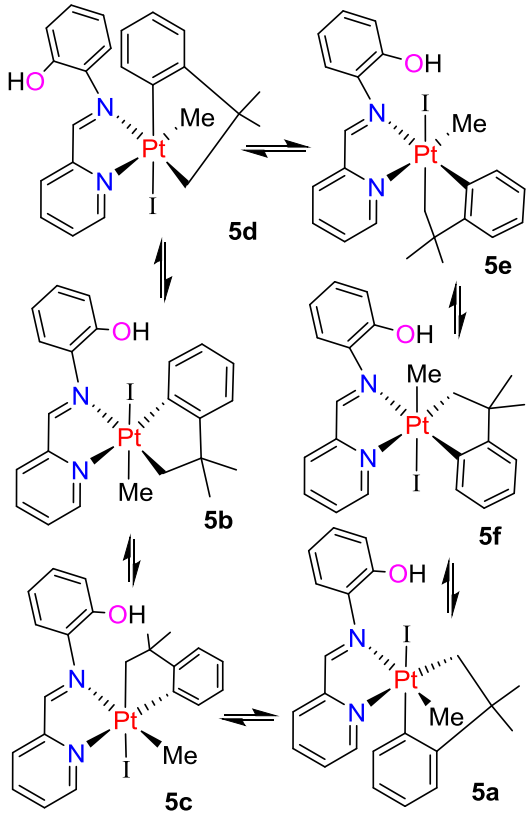

Scheme 4. Likely sequence of reactions to form complex **5a**.

complex **2** the OH Pt hydrogen bond may block approach of methyl iodide on the side *syn* to the phenol group, so the kinetic product might be expected to be **6b′**, formed by approach of MeI *syn* to the NH group. If the complexes isomerize through the iodide dissociation mechanism, the iodide is expected to switch between being *syn* and *anti* to the NH group in each step, as illustrated in Scheme 5. Thus **6b** would give **6c′** and then **6a** while, similarly, **6b′** would give **6c** and then **6a'**. However, if the weaker amine donor can dissociate reversibly, inversion at nitrogen and re-coordination could allow formation of all isomers.

2.3. Oxidative addition of hydrogen peroxide

The reactions of complexes **1**–**4** with hydrogen peroxide are shown in Scheme 6, giving the platinum (IV) products **9**–**12**. In these reactions the products were formed selectively, and the problems associated with isomeric mixtures observed in oxidative addition with methyl iodide were not observed. However, the products were not easy to crystallize and only the structure of complex **12** was determined crystallographically (Fig. 8). Complex **12** is the product of *trans* oxidative addition and is expected from the stepwise polar mechanism of reaction [4–6,12–15,22]. The complex forms a supramolecular polymer in the crystalline state through multiple hydrogen bonding interactions (Fig. 8). On one side of each molecule there are equivalent head-to-tail NH OH(Pt) hydrogen bonds [N (2) O (1A) = O (1) N (2A) 2.80 (2) Å], and on the other side there are equivalent strong phenol COH OH(Pt) hydrogen bonds [O (2) O (3B) = O (3) O (2B) 2.58 (2) Å]. The neighboring equivalent molecules are related by inversion symmetry so, although molecules of **12** are chiral, each polymer chain is racemic.

A feature of the ^{1}H NMR spectrum of **12** is that the protons of the CH_2 groups are non-equivalent and give rise to an 'AB' quartet

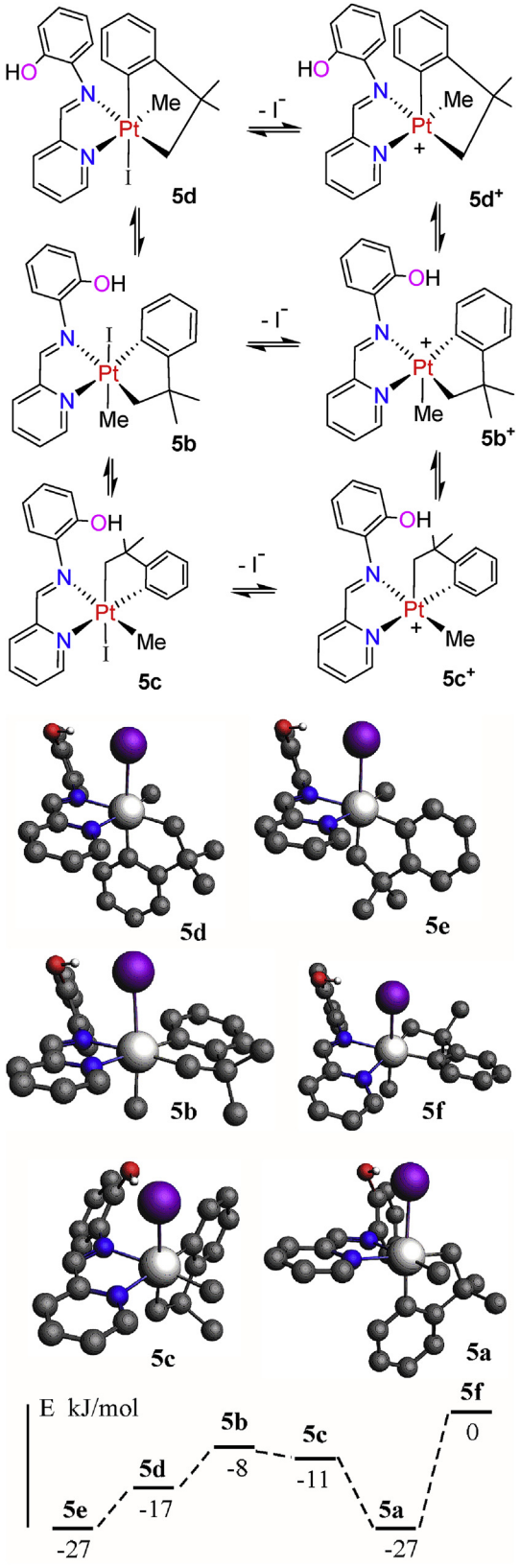

Fig. 6. The calculated structures and relative energies (kJ mol^{-1} with respect to the least stable isomer **5f**) of the six possible isomers of complex **5**.

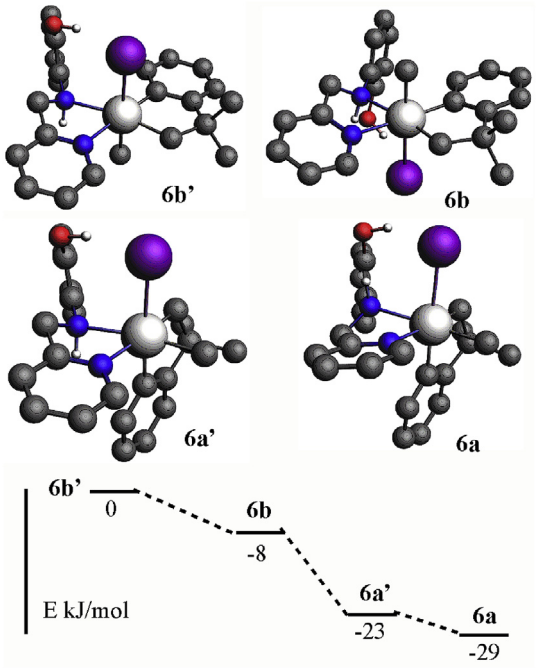

Fig. 7. Calculated structures and relative energies (kJ/mol with respect to the least stable isomer **6b**′) of selected isomers of complex **6**. Selected distances: **6a**, NH I 2.95, OH I 2.75; **6a**′, NH I 4.67, OH I 2.50; **6b**, NH I 2.35, OH I 2.71; **6b**′, NH I 4.66, OH I 2.50 Å.

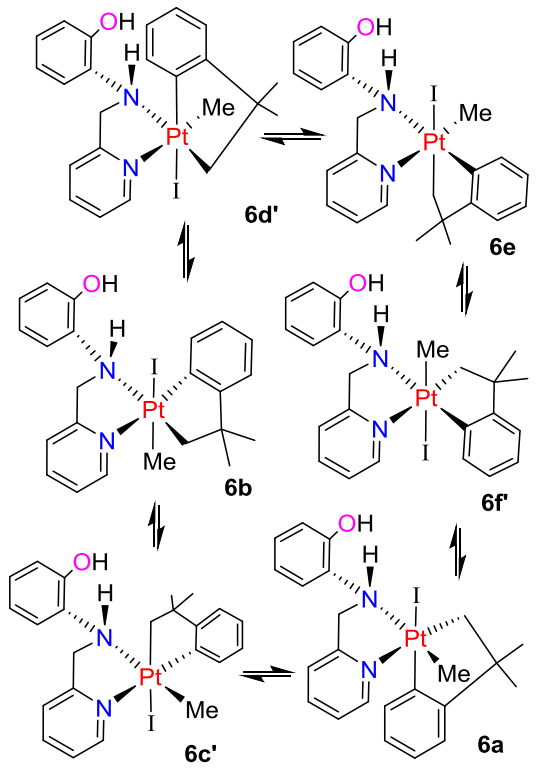

Scheme 5. Predicted isomers of **6**, arising from the iodide dissociation mechanism from complex **6b**.

pattern [$\delta(CH^AH^BN) = 5.12$ and 4.83, ^2J $(H^AH^B) = 15$ Hz); $\delta(CH^AH^BPt) = 3.86$ and 3.57, ^2J $(H^AH^B) = 7$ Hz], and the Me_2C group gives two methyl resonances [$\delta(CMe^AMe^BC) = 1.37$ and 1.36]. These features arise necessarily from the presence of the asymmetry at

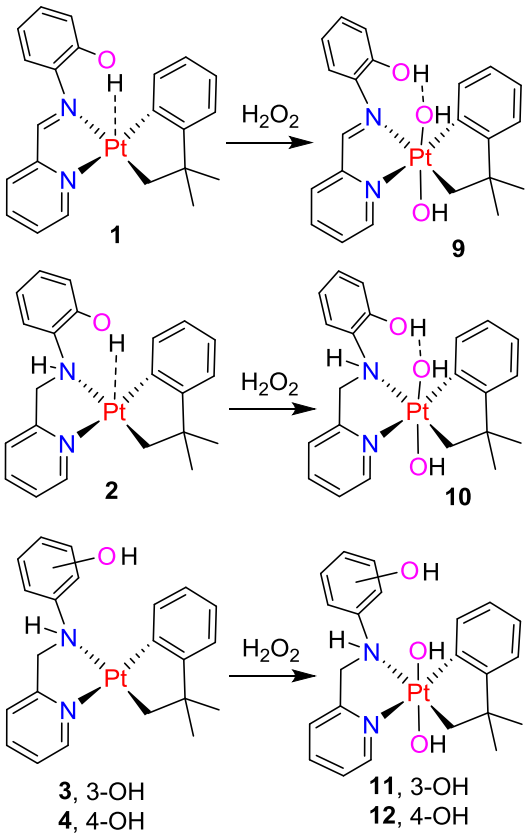

Scheme 6. Reactions with hydrogen peroxide.

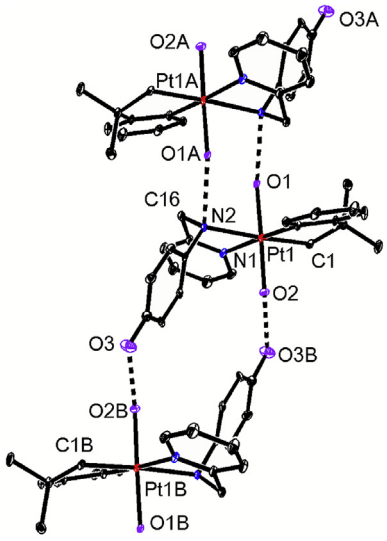

Fig. 8. A view of the structure of complex **12**, showing 30% probability ellipsoids. Selected bond parameters: Pt (1)C (1) 2.063 (9), Pt (1)C (6) 2.007 (8), Pt (1)N (1) 2.170 (7), Pt (1)N (2) 2.254 (7), Pt (1)O (1) 2.043 (6), Pt (1)O (2) 2.018 (6) Å; C (2)Pt (1)C (7) 82.29 (13), N (1)Pt (1)N (2) 77.24 (10) °. H-bond distances: N (2) O (1A) = O (1) N (2A) 2.80 (2), O (2) O (3B) = O (3) O (2B) 2.58 (2) Å. Equivalent positions: x, y, z; A, 1-x, 1-y, 1-z; B, 1-x, 1-y, 2-z.

the amine nitrogen atom, and the ^{1}H NMR spectra of the amine derivatives **10** and **11** display similar features (see experimental section). The imine complex **9** gives the same features for the cycloneophyl resonances in the ^{1}H NMR spectrum [$\delta(CH^{A}H^{B}Pt) = 4.29$ and 3.75, $^{2}J(H^{A}H^{B}) = 7$ Hz; $\delta(CMe^{A}Me^{B}C) = 1.43$ and 1.34]. In this case, the non-equivalence indicates that the intramolecular hydrogen bond (Scheme 6) is sufficiently strong that easy rotation of the phenol substituent, leading to mirror symmetry, does not occur. An alternative explanation for the 2-phenol derivatives **9** and **10** is that chelation of the phenol group leads to the structure **A** or **B** (Fig. 9). DFT calculations predict that **9** is the preferred product by 87 kJ mol^{-1} (Fig. 9). The predicted preference for **10** is lower but we note that the analogous dimethylplatinum (IV) complex is formed as [Pt $(OH)_2Me_2$ (**L2**)] [22]. The DFT calculations predict a strong intramolecular hydrogen bond in both **9** and **10**, with d (O O) 2.48 and 2.51 Å in **9** and **10** respectively (Fig. 9).

3. Conclusions

The oxidative addition reactions of methyl iodide and hydrogen peroxide to the cycloneophylplatinum (II) complexes **1**–**4** are thought to occur by a polar mechanism, but the observed products have different stereochemistries. Hydrogen peroxide is suggested to give selective *trans* oxidative addition (Scheme 6) in all cases, though the structure is only proved crystallographically for complex **12** (Fig. 8), and this selectivity is consistent with most previous studies of platinum (II) complexes [4,12–15,22,27–30]. The oxidative addition of methyl iodide is also likely to occur with *trans* stereochemistry but, in this case, isomerization of the initially formed isomer(s) can occur and for complex **6** the rate of isomerization is competitive with the rate of oxidative addition. The isomers isolated in crystalline form were those of *cis* oxidative addition, whose formation from the expected kinetic product requires two isomerization steps (Schemes 3–5).

4. Experimental

4.1. Reagents and general procedures

The precursor complex $[Pt_2(CH_2CMe_2C_6H_4)_2(\mu\text{-}SMe_2)_2]$ and the platinum (II) complexes **1**–**4** were prepared by the literature methods [21,31]. NMR spectra were recorded using a Varian Inova 600 MHz spectrometer. Complete assignments were aided by the use of ^{1}H–^{1}H gCOSY, ^{1}H–^{13}C HSQC, and ^{1}H–^{13}C HMBC experiments

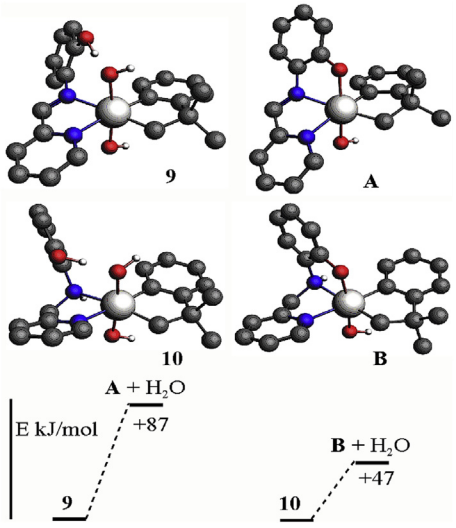

Fig. 9. The calculated structures and relative energies of complexes **9** vs. **A** and **10** vs. **B**. Selected distances (Å): **9**, CO–H 1.08, *syn*-PtO-H 0.98, COH OH(Pt) 1.41, CO OPt 2.48; **10**, CO–H 1.06, *syn*-PtO-H 0.98, COH OH(Pt) 1.47, CO OPt 2.51.

and are reported using the labeling scheme in Chart 2. Typical spectra are shown in the Supporting Information. MALDI-TOF mass spectra were collected using an AB Sciex 5800 TOF/TOF mass spectrometer using pyrene or anthracene as the matrix in a 20:1 matrix:substrate molar ratio. IR spectra were recorded by using a PerkinElmer UATR TWO FTIR spectrometer.

Single-crystal X-ray diffraction measurements were made using a Bruker APEX-II CCD diffractometer with graphite-monochromated Mo Kα (λ = 0.71073 Å) radiation. Single crystals of the complexes were immersed in paraffin oil and mounted on MiteGen micromounts. The structures were solved using direct methods and refined by the full-matrix least-squares procedure of SHELXTL. All heavy atoms were refined anisotropically. The hydrogen atoms were introduced at idealized positions and were treated using the riding model. This treatment (AFIX 83 in SHELXTL) can lead to ambiguity in the positions of H-atoms of hydroxyl groups, and so the OH bond parameters are not discussed. Crystallographic data are given in the crystallographic information files (CCDC 1938859–1938863, 1939296) and a summary of the data is given in the Supporting Information (Table S1).

4.2. Synthetic procedures

4.2.1. [PtIMe($CH_2CMe_2C_6H_4$) (L1)], 5a

To a solution of complex **1** (0.100 g, 0.190 mmol) in CH_2Cl_2 (10 mL) at room temperature was added MeI (23 μL, 0.38 mmol). The reaction mixture was stirred for 2 h and the white precipitate which formed was separated by filtration, washed with hexane (3 × 2 mL) and CH_2Cl_2 (3 × 2 mL) and dried under vacuum, to give complex **5a** (0.079 g, 0.118 mmol, 63%). NMR in $(CD_3)_2SO$: δ(^{1}H) 9.18 (s, 1H, $^3J_{PtH}$ = 33 Hz, *H*7a), 9.08 (d, 1H, $^3J_{PtH}$ = 16 Hz, *J* = 5 Hz, *H*6a), 8.41–8.42 (m, 2H, *H*3a, *H*4a), 8.01 (dd, 1H, *J* = 5 Hz, 8 Hz, *H*5a), 7.35 (d, 1H, *J* = 8 Hz, *H*6b), 7.04 (t, 1H, *J* = 8 Hz, *H*4b), 6.79–6.81 (m, 2H, *H*3b, *H*5b), 6.69 (t, 1H, *J* = 7 Hz, *H*4), 6.50 (d, 1H, *J* = 7 Hz, *H*3), 6.44 (t, 1H, *J* = 7 Hz, *H*5), 5.52 (d, 1H, *J* = 7 Hz, J_{PtH} = 55 Hz, *H*6), 2.72–2.78 (m, 2H, *H*8, *H*8′), 1.47 (s, 3H, J_{PtH} = 72 Hz, *Me*Pt), 1.03 (s, 3H, *H*9), 0.46 (s, 3H, *H*9′); δ(^{13}C) 170.42 (*C*7a), 161.30 (*C*2), 154.49 (*C*2a), 148.31 (*C*2b), 140.09 (*C*6a), 142.50 (*C*1), 140.86 (*C*4a), 134.45 (*C*1b), 131.25 (*C*3a), 129.86 (*C*5a), 128.89 (*C*4b), 126.78 (*C*6), 125.77 (*C*6b), 125.41 (*C*5), 124.49 (*C*4), 124.35 (*C*3), 48.14 (*C*7), 35.26 (*C*9), 35.16 (*C*8), 32.62 (*C*9'), −7.81 (*Me*Pt). Single crystals suitable for X-ray crystallographic analysis were grown by the slow evaporation of an acetone solution of **5**.

Crystalline samples of complexes **6a**, **7a** and **8a** were prepared similarly from complexes **2**, **3** and **4** respectively. Anal. Calc. for $C_{23}H_{27}IN_2OPt$: C, 41.26; H, 4.06; N, 4.18. Found for **6a**: C, 41.39; H, 4.41; N, 4.05. Found for **7a**: C, 41.52; H, 4.16; N, 3.93. Found for **8a**: C, 41.69; H, 4.28; N, 4.39%.

4.2.2. [PtI(CD_3) ($CH_2CMe_2C_6H_4$(L1)], 5b-d_3

An NMR tube containing a solution of **1** (0.025 g, 0.047 mmol) in CD_2Cl_2 (1.5 mL) was inserted in NMR instrument and the probe was cooled to −30 °C. A proton spectrum of **1** was collected at −30 °C, then the NMR tube was ejected and CD_3I (2eq, 6 μL) was added and the NMR tube was inserted immediately. An immediate proton NMR was collected. Afterward, the probe was slowly warmed up until no starting complex was observed. At 0 °C mostly **5b-*d*$_3$** was observed and full NMR characterization was carried out at this temperature. NMR in CD_2Cl_2 at 0 °C: δ(^{1}H) 8.97 (d, 1H, $^3J_{PtH}$ = 15 Hz, *J* = 6 Hz, *H*6a), 8.91 (s, 1H, $^3J_{PtH}$ = 24 Hz, *H*7a), 8.17 (t, 1H, *J* = 8 Hz, *H*4a), 8.12 (d, 1H, *J* = 8 Hz, *H*3a), 7.77 (dd, 1H, *J* = 8 Hz, 6 Hz, *H*5a), 7.41 (t, 1H, *J* = 8 Hz, *H*5b), 7.13 (d, 1H, *J* = 8 Hz, *H*6b), 7.05 (t, 1H, *J* = 8 Hz, *H*4b), 7.01 (d, 1H, *J* = 8 Hz, *H*3b), 6.76 (t, 1H, *J* = 8 Hz, *H*4), 6.68 (d, 1H, *J* = 8 Hz, *H*3), 6.46 (t, 1H, *J* = 8 Hz, *H*5), 6.25 (d, *J* = 8 Hz, $^3J_{PtH}$ = 36 Hz, *H*6), 4.06 (d, 1H, *J* = 8 Hz, J_{PtH} = 125 Hz, *H*8), 3.21 (d, 1H, *J* = 8 Hz, J_{PtH} = 72 Hz, *H*8′), 1.42 (s, 3H, *H*9), 1.26 (s, 3H, *H*9′). ^{13}C {^{1}H} NMR (CD_2Cl_2, 151 MHz, 0 °C) δ: 169.36 (*C*7a), 164.90 (*C*2), 153.74 (*C*2a), 152.40 (*C*2b), 149.27 (*C*6a), 149.26 (*C*1), 139.86 (*C*4a), 130.76 (*C*3a), 130.18 (*C*5b), 129.06 (*C*5a), 128.73 (*C*6), 124.61 (*C*5), 124.33 (*C*3), 124.11 (*C*4), 123.67 (*C*1b), 122.72 (*C*3b), 120.71 (*C*4b), 117.97 (*C*6b), 43.78 (*C*7), 40.08 (*C*8), 33.97 (*C*9'), 31.60 (*C*9). Warming the solution to 0 °C resulted in precipitate formation, which was dissolved in DMSO and confirmed to be **5a**.

The reactions of **2**, **3** and **4** with CD_3I were carried out in a similar way to give **6b**, **7b** and **8b** as major isomers. **6b**, NMR in CD_2Cl_2 at −30 °C: δ(^{1}H) 8.51 (d, 1H, *J* = 6 Hz, *H*6a), 7.90 (d, 1H, *J* = 8 Hz, *H*3a), 7.47–7.50 (m, 2H, *H*4a, *H*5a), 7.41 (t, 1H, *J* = 8 Hz, *H*5b), 7.13 (d, 1H, *J* = 8 Hz, *H*6b), 6.82 (t, 1H, *J* = 8 Hz, *H*4), 6.75–6.79 (m, 3H, *H*3b, *H*6b, *H*5), 6.55 (d, 1H, *J* = 8 Hz, *H*3), 6.46 (t, 1H, *J* = 8 Hz, *H*5b), 6.35 (d, 1H, *J* = 8 Hz, *H*6), 4.85 (d, 1H, *J* = 15 Hz, *H*7a), 4.62 (d, 1H, *J* = 15 Hz, *H*7a′), 2.54 (d, 1H, *J* = 8 Hz, *H*8), 1.91 (d, 1H, *J* = 8 Hz, *H*8′), 1.36 (s, 3H, *H*9), 1.19 (s, 3H, *H*9′). **7b**, NMR in CD_2Cl_2 at −30 °C: δ(^{1}H) 8.61 (d, 1H, *J* = 6 Hz, *H*6a), 8.20 (d, 1H, *J* = 8 Hz, *H*3a), 7.71 (t, 1H, *J* = 8 Hz, *H*4a), 7.27 (t, 1H, *J* = 8 Hz, *H*5b), 6.80–6.82 (m, 2H, *H*5a, *H*4b), 6.62 (m, 1H, *H*6b), 6.58 (s, 1H, *H*2b), 6.25 (d, 1H, *J* = 8 Hz, *H*3), 5.72–5.75 (m, 2H, *H*4, *H*5), 5.00 (d, 1H, *J* = 8 Hz, *H*6), 4.00 (d, 1H, *J* = 15 Hz, *H*7a), 3.04 (d, 1H, *J* = 15 Hz, *H*7a′), 2.25 (d, 1H, *J* = 8 Hz, *H*8), 1.81 (d, 1H, *J* = 8 Hz, *H*8′), 1.36 (s, 3H, *H*9), 1.24 (s, 3H, *H*9′). **8b**, NMR in CD_2Cl_2 at −30 °C: δ(^{1}H) 8.37 (d, 1H, *J* = 8 Hz, *H*6), 8.01–8.09 (m, 2H, *H*3a, *H*4a), 7.86 (d, 1H, *J* = 6 Hz, *H*6a), 7.43 (t, 1H, *J* = 8 Hz, *H*5a), 7.17 (d, 2H, *J* = 8 Hz, *H*2b, *H*6b), 6.89 (d, 2H, *H*3a, *H*5b), 6.87–6.88 (m, 2H, *H*3, *H*4), 6.76 (t, 1H, *J* = 8 Hz, *H*5), 5.39 (d, 1H, *J* = 15 Hz, *H*7a), 5.18 (d, 1H, *J* = 15 Hz, *H*7a′), 2.77 (d, 1H, *J* = 9 Hz, *H*8), 2.26 (d, 1H, *J* = 9 Hz, *H*8′), 1.11 (s, 3H, *H*9), 0.72 (s, 3H, *H*9').

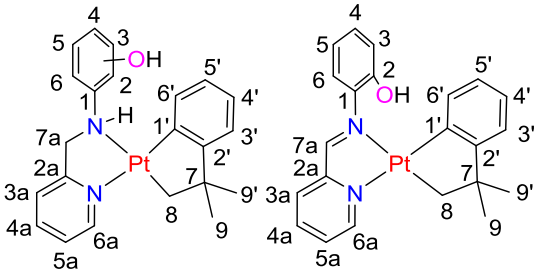

Chart 2. NMR labelling scheme.

4.2.3. [Pt(OH)$_2$($CH_2CMe_2C_6H_4$) (L1)], 9

To a stirred solution of complex **1** (0.108 g, 0.208 mmol) in CH_2Cl_2 (10 mL) was added H_2O_2 (2 eq, 37 μL). After 20 min the volume was reduced to 3 mL, and hexane (10 mL) was added to precipitate the product, which was filtered, washed with hexane (3 × 2 mL) and ether (3 × 2 mL), and dried under vacuum. Yield 0.085 g, 0.157 mmol, 76%. NMR in CD_2Cl_2: δ(^{1}H) 9.02 (s, *1H, H*7a), 8.92 (d, 1H, J_{PtH} = 15 Hz, *J* = 5 Hz, *H*6a), 8.14 (t, 1H, *J* = 7 Hz, *H*4a), 8.08 (d, 1H, *J* = 7 Hz, *H*3a), 7.77 (m, *H*5a), 7.38 (t, 1H, *J* = 8 Hz, *H*4b), 7.20 (d, 1H, *J* = 8 Hz, *H*6b), 7.02 (t, 1H, *J* = 8 Hz, *H*5b), 6.94 (d, 1H, *J* = 8 Hz, *H*3b), 6.90 (t, *J* = 8 Hz, *H*4), 6.78 (d, 1H, *J* = 8 Hz, *H*3), 6.53 (t, 1H, *J* = 8 Hz, *H*5), 6.42 (d, 1H, *J* = 8 Hz, *H*6), 4.29 (d, 1H, *J* = 7 Hz, J_{PtH} = 84 Hz, *H*8), 3.75 (d, 1H, *J* = 7 Hz, J_{PtH} = 84 Hz, *H*8′), 1.43 (s, 3H, *H*9), 1.34 (s, 3H, *H*9′); δ(^{13}C) 168.23 (*C*7a), 162.29 (*C*2), 153.05 (*C*2a), 151.96 (*C*2b), 149.04 (*C*6a), 140.40 (*C*5a), 137.75 (*C*1b), 130.24 (*C*4b), 129.91 (*C*6 *and* *C*3a), 128.90 (*C*4a), 126.91 (*C*1), 128.90 (*C*4), 124.93 (*C*5), 124.20 (*C*3), 121.34 (*C*3b), 119.54 (*C*5b), 118.34 (*C*6b), 43.76 (*C*7), 41.98 (*C*8), 33.69 (*C*9), 32.89 (*C*9').

4.2.4. [Pt(OH)$_2$($CH_2CMe_2C_6H_4$) (L2)], 10

This was prepared similarly from complex **2** and H_2O_2. NMR in

CD_2Cl_2: δ(^{1}H) 8.70 (d, 1H, $J = 5$ Hz, *H*6a), 8.09 (t, 1H, $J = 7$ Hz, *H*4a), 7.76 (d, 1H, $J = 7$ Hz, *H*3a), 7.60 (dd, 1H, $J = 5$ Hz, 7 Hz, *H*5a), 7.43 (d, 1H, $J = 8$ Hz, *H*6b), 7.11 (t, 1H, $J = 8$ Hz, *H*4), 6.75–6.79 (m, 3H, *H*3b, *H*4b, *H*5b), 6.70 (d, 1H, $J = 8$ Hz, *H*3), 6.38 (t, 1H, $J = 8$ Hz, *H*5), 6.26 (d, 1H, $J = 8$ Hz, *H*6), 5.33 (dd, 1H, $J = 15$ Hz, 10 Hz, *H*7a), 4.68 (dd, 1H, $J = 15$ Hz, 3 Hz, *H*7a′), 3.78 (d, 1H, $J = 7$ Hz, $J_{PtH} = 84$ Hz, *H*8), 3.42 (d, 1H, $J = 7$ Hz, $J_{PtH} = 84$ Hz, *H*8′), 1.33 (s, 3H, *H*9), 1.32 (s, 3H, *H*9′). ^{13}C {^{1}H} NMR (CD_2Cl_2, 151 MHz, 25 °C) δ: 163.24 (*C*2), 159.58 (*C*2a), 153.09 (*C*2b), 147.77 (*C*6a), 139.64 (*C*4a), 134.24 (*C*1b), 129.92 (*C*6), 127.38 (*C*4), 125.31 (*C*3b), 124.51 (*C*5a), 124.39 (C5), 124.22 (*C*6b), 123.46 (*C*3), 123.01 (*C*3a), 120.45 (*C*4b), 118.83 (*C*5b), 55.39 (*C*7a), 44.05 (*C*7), 40.88 (C8), 29.82 (*C*9), 23.66 (*C*9').

4.2.5. [Pt(OH)$_2$(CH$_2$CMe$_2$C$_6$H$_4$) (L3)], 11

This was prepared similarly from complex **3** and H_2O_2. NMR in CD_2Cl_2: δ(^{1}H) 8.78 (d, 1H, $J = 5$ Hz, *H*6a), 8.15 (t, 1H, $J = 7$ Hz, *H*4a), 7.84 (d, 1H, $J = 7$ Hz, *H*3a), 7.67 (dd, 1H, $J = 7$ Hz, 5Hz, *H*5a), 7.23 (t, 1H, $J = 8$ Hz, *H*5b), 6.92 (s, 1H, *H*2b), 6.76 (d, 1H, $J = 8$ Hz, *H*4b), 6.91 (d, 1H, $J = 8$ Hz, *H*6b), 6.90 (t, 1H, $J = 8$ Hz, *H*4), 6.85 (d, 1H, $J = 8$ Hz, *H*3), 6.76 (d, 1H, $J = 8$ Hz, *H*3b), 6.53 (t, 1H, $J = 8$ Hz, *H*5), 6.33 (d, 1H, $J = 8$ Hz, $J_{PtH} = 32$ Hz, *H*6), 5.19 (d, 1H, $J = 15$ Hz, *H*7a), 4.85 (d, 1H, $J = 15$ Hz, *H*7a'), 3.89 (d, 1H, $J = 7$ Hz, $J_{PtH} = 88$ Hz, *H*8a), 3.42 (d, 1H, $J = 7$ Hz, $J_{PtH} = 82$ Hz, *H*8b), 1.38 (s, 3H, *H*9a), 1.36 (s, 3H, *H*9b). ^{13}C {^{1}H} NMR (CD_2Cl_2, 151 MHz, 25 °C) δ: 164.70, 161.53, 159.95, 149.56, 149.35, 141.26, 132.24, 131.55, 130.71, 126.69, 126.17, 125.84, 124.47, 113.88, 113.33, 109.42, 58.62, 45.72, 42.24, 34.54, 33.33. Anal. Calc. for $C_{22}H_{26}N_2O_3Pt \cdot H_2O$: C, 45.59; H, 4.87; N, 4.83. Found: C, 45.30; H, 4.77; N, 4.40%.

4.2.6. [Pt(OH)$_2$(CH$_2$CMe$_2$C$_6$H$_4$) (L4)], 12

This was prepared similarly from complex **4** and H_2O_2. NMR in CD_2Cl_2: δ(^{1}H) 8.78 (d, 1H, $J = 5$ Hz, *H*6a), 8.13 (t, 1H, $J = 7$ Hz, *H*4a), 7.81 (d, 1H, $J = 7$ Hz, *H*3a), 7.65 (dd, 1H, $J = 7$ Hz, 5Hz, *H*5a), 7.32 (d, 2H, $J = 8$ Hz, *H*2b,6b), 6.84 (t, 1H, $J = 8$ Hz, *H*4), 6.82 (d, 2H, $J = 8$ Hz, *H*3b,5b), 6.76 (d, 1H, $J = 8$ Hz, *H*3), 6.52 (t, 1H, $J = 8$ Hz, *H*5), 6.29 (d, 1H, $J = 8$ Hz, $J_{PtH} = 32$ Hz, *H*6), 5.12 (d, 1H, $J = 15$ Hz, *H*7a), 4.83 (d, 1H, $J = 15$ Hz, *H*7a′), 3.86 (d, 1H, $J = 7$ Hz, $J_{PtH} = 88$ Hz, *H*8), 3.57 (d, 1H, $J = 7$ Hz, $J_{PtH} = 80$ Hz, *H*8′), 1.37 (s, 3H, *H*9), 1.36 (s, 3H, *H*9′). ^{13}C {^{1}H} NMR (CD_2Cl_2, 151 MHz, 25 °C) δ: 165.01 (C2), 161.63 (C2a), 156.78 (C4b), 149.68 (C6a), 141.35 (C4a), 140.24 (C1b), 132.46 (C1), 130.87 (C6), 126.78 (C4), 126.28 (C5a), 125.84 (C5), 125.16 (C3), 124.50 (C3a), 123.93(C2b, C6b), 117.29 (C3b, C5b), 59.93 (C7a), 45.81 (C7), 41.93 (C8), 34.88 (C9), 33.49 (C9'). Anal. Calc. for $C_{22}H_{26}N_2O_3Pt \cdot H_2O$: C, 45.59; H, 4.87; N, 4.83. Found: C, 45.40; H, 4.55; N, 4.65%.

Acknowledgment

We thank the NSERC (Canada) for financial support.

Appendix A. Supplementary data

Supplementary data to this article can be found online at https://doi.org/10.1016/j.jorganchem.2019.120962.

References

[1] R.H. Crabtree, The Organometallic Chemistry of the Transition Elements, seventh ed., Wiley, 2019.
[2] D. Astruc, Organometallic Chemistry and Catalysis, Springer, 2007.
[3] J.F. Hartwig, Organotransition Metal Chemistry: from Bonding to Catalysis, University Science Books, 2010.
[4] L.M. Rendina, R.J. Puddephatt, Chem. Rev. 97 (1997) 1735–1754.
[5] M. Crespo, M. Martinez, S.M. Nabavizadeh, M. Rashidi, Coord. Chem. Rev. 279 (2014) 115–140.
[6] M. Crespo, R.J. Puddephatt, Organometallics 6 (1987) 2548–2550.
[7] Z. Du, Z. Shao, Chem. Soc. Rev. 42 (2013) 1337–1378.
[8] M. Raynal, P. Ballester, A. Vidal-Ferran, P.W.N.M. van Leeuwen, Chem. Soc. Rev. 43 (2014) 1660–1733.
[9] S. Afewerki, A. Cordova, Chem. Rev. 116 (2016) 13512–13570.
[10] D.-S. Kim, W.-J. Park, C.-H. Jun, Chem. Rev. 117 (2017) 8977–9015.
[11] M.E. Moustafa, P.D. Boyle, R.J. Puddephatt, Chem. Commun. 51 (2015) 10334–10336.
[12] M.A. Fard, A. Behnia, R.J. Puddephatt, Organometallics 36 (2017) 4169–4178.
[13] K.A. Thompson, C. Kadwell, P.D. Boyle, R.J. Puddephatt, J. Organomet. Chem. 829 (2017) 22–30.
[14] A. Abo-Amer, P.D. Boyle, R.J. Puddephatt, Inorg. Chim. Acta 473 (2018) 51–59.
[15] V.V. Rostovtsev, L.M. Henling, J.A. Labinger, J.E. Bercaw, Inorg. Chem. 41 (2002) 3608–3619.
[16] E.M. Prokopchuk, H.A. Jenkins, R.J. Puddephatt, Organometallics 18 (1999) 2861–2866.
[17] C.S.A. Fraser, M.C. Jennings, R.J. Puddephatt, Chem. Commun. (2001) 1310–1311.
[18] M.A. Fard, A. Behnia, R.J. Puddephatt, Can. J. Chem. 97 (2019) 238–243.
[19] M.S. McCready, R.J. Puddephatt, ACS Omega 3 (2018) 13621–13629.
[20] F. Zhang, M.C. Jennings, R.J. Puddephatt, Chem. Commun. (2007) 1496–1498.
[21] A. Behnia, M.A. Fard, P.D. Boyle, R.J. Puddephatt, Eur. J. Inorg. Chem. (2019) 2899–2906.
[22] M.A. Fard, A. Behnia, R.J. Puddephatt, ACS Omega 4 (2019) 257–268.
[23] M.A. Fard, A. Behnia, R.J. Puddephatt, J. Organomet. Chem. 890 (2019) 32–42.
[24] T. Steiner, Acta Crystallogr. B54 (1998) 456–463.
[25] L. Brammer, E.A. Bruton, P. Sherwood, Cryst. Growth Des. 1 (2001) 277–290.
[26] R.J. Puddephatt, Can. J. Chem. 97 (2019) 529–537.
[27] K. Thorshaug, I. Fjeldahl, C. Romming, M. Tilset, Dalton Trans. (2003) 4051–4056.
[28] M. Rashidi, M. Nabavizadeh, R. Hakimelahi, S. Jamali, Dalton Trans. (2001) 3430–3434.
[29] R.A. Taylor, D.J. Law, G.J. Sunley, A.J.P. White, G.J.P. Britovsek, Chem. Commun. (2008) 2800–2802.
[30] B. Lippert, P.J.S. Miguel, Coord. Chem. Rev. 327 (2016) 333–348.
[31] M.A. Fard, A. Behnia, R.J. Puddephatt, Organometallics 37 (2018) 3368–3377.